J. Phys. B: At. Mol. Opt. Phys. **31** (1998) 449–464. Printed in the UK PII: S0953-4075(98)86731-X

# On the influence of pulse shapes on ionization probability

C Figueira de Morisson Faria†§, A Fring‡∥ and R Schrader‡¶

† Max-Born-Institut, Rudower Chaussee 6, D-12474 Berlin, Germany

‡ Institut für Theoretische Physik, Freie Universitat Berlin, Arnimallee 14, D-14195 Berlin, Germany

Received 11 August 1997, in final form 9 October 1997

**Abstract.** We investigate analytical expressions for the upper and lower bounds for the ionization probability through ultra-intense short-pulse laser radiation. We take several different pulse shapes into account, including, in particular, those with a smooth adiabatic turn-on and turn-off. For all situations for which our bounds are applicable we do not find any evidence for bound-state stabilization.

## 1. Introduction

The computation of ionization rates or probabilities of atoms through low-intensity ($I \ll 3.5 \times 10^{16}$ W cm$^{-2}$) laser radiation can be carried out successfully using perturbation theory around the solution of the Schrödinger equation without the presence of laser fields [1]. With the advance of laser technology, nowadays intensities of up to $10^{19}$ W cm$^{-2}$ are possible and pulses may be reduced to a duration of ($\tau \sim 10^{-15}$ s)+. Such intensities are no longer in the region of validity of conventional perturbation theory. The new regime is usually tackled by perturbative methods around the Gordon–Volkov solution [3] of the Schrödinger equation [4–10], fully numerical solutions of the Schrödinger equation [11–16], Floquet solution [17–19], high-frequency approximations [20] or analogies to classical [21] and semiclassical [22] dynamical systems. All these methods have their drawbacks. The most surprising outcome of the analysis of the high-intensity region for short pulses (the pulse length is shorter than 1 ps) is the finding by the majority of the atomic physics community (see [23–26] and references therein) of so-called atomic stabilization. This means that the probability of ionization by a pulse of laser radiation, which for low intensities increases with increasing intensities, reaches some sort of maximum at high intensities and commences to decrease until ionization is almost totally suppressed. This picture is very counterintuitive and doubts on the existence of this phenomenon have been raised by several authors [7, 9, 10, 27, 28], who do not find evidence for it in their computations. So far no support is given to either side by experimentalists*. For reviews on the subject we refer the reader to [23–26].

§ E-mail address: Faria@mbi-berlin.de

∥ E-mail address: Fring@physik.fu-berlin.de

¶ E-mail address: Schrader@physik.fu-berlin.de

+ For a review and the experimental realization of such pulses see, for instance, [2].

* Experimental evidence for some sort of stabilization is given in [29], but these experiments deal with intensities of $10^{13}$ W cm$^{-2}$, which is not the 'ultra-intense' regime for which the theoretical predictions are made.

0953-4075/98/030449+16$19.50  

Since all of the above methods involve a high degree of numerical analysis, which are difficult to be verified by third parties, it is extremely desirable to reach some form of analytical understanding. In [30–33] we derived analytical expressions for upper and lower bounds for the ionization probability, meaning that the ionization probability is certainly lower or higher, respectively, than these values. The lower bound, in particular, may be employed to investigate the possibility of stabilization for an atomic bound state. In [33] we analysed the hydrogen atom and found that for increasing intensities the lower bound also increases and hence that the existence of atomic stabilization can be excluded in the sense that the ionization probability tends to one. The shortcoming of our previous analysis [33] is that definite conclusions concerning the above question may only be reached for extremely short pulses ($\tau < 1$ au), which are experimentally unrealistic. In the present paper we analyse these bounds in further detail and demonstrate that atomic stabilization can also be excluded for longer pulses.

Some authors [8, 14] put forward the claim that in order to 'observe' atomic stabilization one requires pulses which are switched on, sometimes also off, smoothly. This seems very surprising since stabilization is supposed to be a phenomenon specific to high intensities and with these types of pulses emphasis is just put on the importance of the low-intensity regime. It further appears that among the authors who put forward these claims, it is not commonly agreed upon whether one should associate these pulse shapes with the laser field or the associated vector potential. We did not find a proper and convincing physical explanation as to why such pulses should produce such surprising effects in the literature. Geltman [10] and also Chen and Bernstein [27] do not find evidence for stabilization for these types of pulses with smooth turn on (and off) of the laser field. However, these results have also been disputed (Su *et al* 1996 [14]) with regard to numerical convergence problems [10] and the possibility to allow distortions of the electron trajectory, which is believed to be necessary for the occurrence of stabilization [27].

In order to also address the validity of these claims within our framework we extend our previous analysis to various types of pulses commonly employed in the literature in this context and also investigate the effects that different frequencies might have. Once more we conclude that our arguments do not support atomic stabilization.

Our paper is organized as follows. In section 2 we briefly recall the principle of our argument and our previous expressions for the upper and lower bounds for the ionization probability and discuss them in more detail for the hydrogen atom. We then turn to an analysis for specific pulses. In section 3 we state our conclusions. In the appendix we present the explicit computation for the Hilbert space norm of the difference of the potential in the Kramers–Henneberger frame and the one in the laboratory frame for any bound state.

## 2. The upper and lower bounds

For the convenience of the reader we commence by summarizing briefly the main principle of our argument. Instead of calculating exact ionization probabilities we compute upper and lower bounds for them, meaning that the exact values are always smaller or greater, respectively. We then vary these bounds with respect to the intensity of the laser field and study their behaviour. If the lower bound tends to one with increasing intensity, we can infer that stabilization is definitely excluded. On the other hand, if the upper bound tends to zero for increasing intensities, we would conclude that stabilization is present. In the case where the lower bound increases, but remains below one, we only take this as an indication for a general type of behaviour and interpret it as not providing any evidence for stabilization, but we cannot definitely exclude its existence. In the case where the lower bound becomes negative or the upper bound becomes greater than one, our expressions obviously do not allow any conclusion.

The non-relativistic quantum mechanical description of a system with potential $V$ in the presence of linearly polarized laser radiation is given by the Schrödinger equation involving the Stark Hamiltonian

$$\mathrm{i}\frac{\partial\psi(\boldsymbol{x},t)}{\partial t} = \left(-\tfrac{1}{2}\Delta + V + z\,E(t)\right)\psi(\boldsymbol{x},t) = H(t)\,\psi(\boldsymbol{x},t). \tag{2.1}$$

For high, but not relativistic, intensities the laser field may be approximated classically. We furthermore assume the dipole approximation. In the following we will always use atomic units $\hbar = e = m_\mathrm{e} = c\alpha = 1$. For a general time-dependent Hamiltonian $H(t)$ the ionization probability of a normalized bound state $\psi$ is defined [6, 30] as

$$P(\psi) = \|(\mathbf{1} - \mathcal{P}_+)S\psi\|^2 = 1 - \|\mathcal{P}_+ S\psi\|^2. \tag{2.2}$$

The gauge invariance of this expression was discussed in [33]. Here $\|\psi\|$ denotes as usual the Hilbert space norm, i.e. $\|\psi\|^2 = \langle\psi,\psi\rangle = \int|\psi(\boldsymbol{x})|^2\,\mathrm{d}^3x$. We always assume that $H_\pm = \lim_{t\to\pm\infty} H(t)$ exists and $\psi$ is then understood to be a bound state of $H_-$. $\mathcal{P}_+$ and $\mathcal{P}_-$ denote the projectors onto the space spanned by the bound states of $H_+$ and $H_-$, respectively, and $S$ is the unitary 'scattering matrix'

$$S = \lim_{t_\pm\to\pm\infty} \exp(\mathrm{i}t_+H_+)\,U(t_+,t_-)\,\exp(-\mathrm{i}t_-H_-). \tag{2.3}$$

Here the unitary time evolution operator $U(t_+,t_-)$ for $H(t)$, brings a state from time $t_-$ to $t_+$. Note that by definition $0 \leqslant P(\psi) \leqslant 1$. Employing methods of functional analysis we derived in [30–33] several analytical expressions by which the possible values for the ionization probability may be restricted. We emphasize once more that these expressions are not to be confused with exact computations of ionization probabilities. We recall here the formula for the upper

$$P_u(\psi) = \left\{\int_0^\tau \|(V(\boldsymbol{x} - c(t)e_z) - V(\boldsymbol{x}))\psi\|\,\mathrm{d}t + |c(\tau)|\|p_z\psi\| + |b(\tau)|\|z\psi\|\right\}^2 \tag{2.4}$$

and the lower bound

$$P_l(\psi) = 1 - \left\{\int_0^\tau \|(V(\boldsymbol{x} - c(t)e_z) - V(\boldsymbol{x}))\psi\|\,\mathrm{d}t \right.$$
$$\left. + \frac{2}{2I_p + b(\tau)^2}\|(V(\boldsymbol{x} - c(t)e_z) - V(\boldsymbol{x}))\psi\| + \frac{2|b(\tau)|}{2I_p + b(\tau)^2}\|p_z\psi\|\right\}^2 \tag{2.5}$$

which were deduced in [33]. $e_z$ is the unit vector in the $z$-direction and $I_p$ is the binding energy. Here we use the notation

$$b(t) := \int_0^t E(s)\,\mathrm{d}s \qquad c(t) := \int_0^t b(s)\,\mathrm{d}s \tag{2.6}$$

for the total classical momentum transfer and the total classical displacement, respectively. Note that for the vector potential in the $z$-direction we have $A(t) = -(1/c)b(t) + \text{constant}$. It is important to recall that the expression for the lower bound is only valid if the classical energy transfer is larger than the ionization energy of the bound state, i.e. $\frac{1}{2}b^2(\tau) > -I_p$. Our bounds hold for all Kato small potentials†. In particular, the Coulomb potential and its modifications, which are very often employed in numerical computations, such as smoothed

† Potentials are called Kato small if for each $a$ with $0 < a < 1$ there is a constant $b < \infty$, such that $\|V\psi\| \leqslant a\|-\Delta\psi\| + b\|\psi\|$ holds for all $\psi$ in the domain $\mathcal{D}(H_0)$ of $H_0 = -\Delta/2$, see for instance [35, 36].

or screened Coulomb potentials, are Kato small. However, the delta potential, which is widely used in toy-model computations because of its nice property of possessing only one bound state, is not a Kato potential.

In the following we will consider a realistic example and take the potential $V$ to be the Coulomb potential and concentrate our discussion on the hydrogen atom. In this case it is well known that the binding energy for a state $\psi_{nlm}$ is $E_n = -1/2n^2$, $\|p_z\psi_{n00}\|^2 = 1/3n^2$ and $\|z\psi_{n00}\|^2 = \frac{1}{3}\langle\psi_{n00}|r^2|\psi_{n00}\rangle = \frac{1}{6}n^2(5n^2+1)$ (see for instance [34]). We will employ these relations below. In [33] it was shown that the Hilbert space norm of the difference of the potential in the Kramers–Henneberger frame [37, 38] and in the laboratory frame applied to the state $\psi$

$$N(\boldsymbol{y}, \psi) := \|(V(\boldsymbol{x}-\boldsymbol{y}) - V(\boldsymbol{x}))\psi\| \tag{2.7}$$

is bounded by 2 when $\psi = \psi_{100}$ for arbitrary $\boldsymbol{y} = ce_z$. We shall now investigate in more detail how this function depends on $c$. In order to simplify notation we ignore in the following the explicit mentioning of $e_z$. In the appendix we present a detailed computation, where we obtain

$$N^2(c, \psi_{100}) = 2 + (1 + |c|^{-1})\mathrm{e}^{-|c|}\,\mathrm{Ei}(|c|) + (1 - |c|^{-1})\mathrm{e}^{|c|}\,\mathrm{Ei}(-|c|) + \frac{2}{|c|}(\mathrm{e}^{-2|c|} - 1). \tag{2.8}$$

Here $\mathrm{Ei}(x)$ denotes the exponential integral function, given by the principal value of the integral

$$\mathrm{Ei}(x) = -\int_{-x}^{\infty} \frac{\mathrm{e}^{-t}}{t}\,\mathrm{d}t \qquad \text{for} \quad x > 0. \tag{2.9}$$

Now considering the asymptotic behaviour of $N$, we obtain as expected $\lim_{c\to 0} N = 0$ and $\lim_{c\to\infty} N = \sqrt{2}$. Noting further that $N$ is a monotonically increasing function of $c$ (one may easily compute its derivatives with respect to $c$, but we refer here only to the

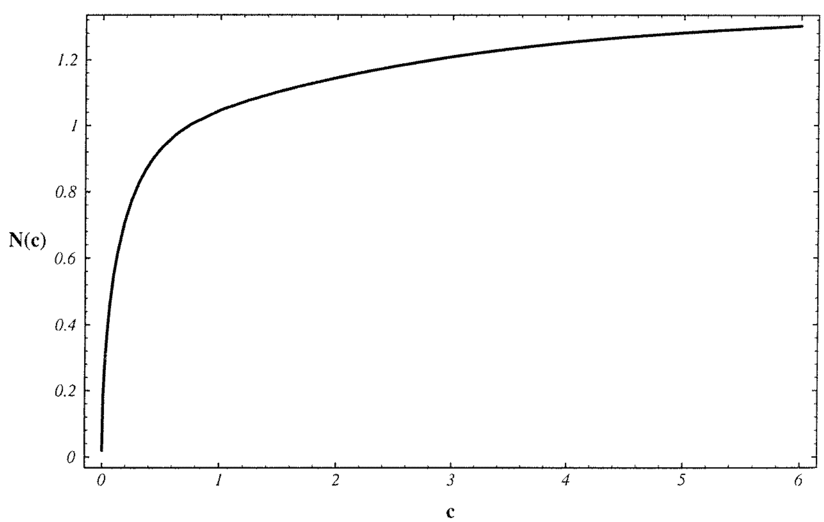


**Figure 1.** The Hilbert space norm of the difference of the potential in the Kramers–Henneberger frame and in the laboratory frame applied to the state $\psi_{100}$ versus the classical displacement $c$.

plot of this function in figure 1), it follows that our previous [33] estimate may, in fact, be improved to $N(c, \psi_{100}) \leqslant \sqrt{2}$. The important thing to notice is that, since $N(c, \psi_{100})$ is an overall increasing function of $c$, it therefore also increases as a function of the field strength. The last term in the bracket of the lower bound $P_l(\psi)$ is a decreasing function of the field strength, while the second term does not have an obvious behaviour. Hence if the first term dominates the whole expression in the bracket, thus leading to a decrease of $P_l(\psi)$, one has in principle the possibility of stabilization. We now investigate several pulse shapes for the possibility of such a behaviour and analyse the expressions

$$P_l(\psi_{100}) = 1 - \left\{ \int_0^\tau N(c(t), \psi_{100})\, \mathrm{d}t + \frac{2N(c(\tau), \psi_{100})}{b(\tau)^2 - 1} + \frac{2}{\sqrt{3}} + \frac{|b(\tau)|}{b(\tau)^2 - 1} \right\}^2 \tag{2.10}$$

$$P_u(\psi_{100}) = \left\{ \int_0^\tau N(c(t), \psi_{100})\, \mathrm{d}t + \frac{|c(\tau)|}{\sqrt{3}} + |b(\tau)| \right\}^2. \tag{2.11}$$

Here we have simply inserted the explicit values for $E_1$, $\|z\psi_{100}\|$ and $\|p_z\psi_{100}\|$ into (2.4) and (2.5), and understand $N(c, \psi_{100})$ to be given by the analytical expression (2.8). The formulae presented in the appendix also allow, in principle, the computation of $N(c, \psi_{nlm})$ for different values of $n, l$ and $m$. However, for $l \neq 0$ the sum over the Clebsch–Gordan coefficients becomes more complicated and due to the presence of the Laguerre polynomial of degree $n$ in the radial wavefunction $R_{nl}$ this becomes a rather complex analytical computation. We will therefore be content with a weaker analytical estimate here. In fact, we have

$$N^2(c(t), \psi_{n00}) \leqslant 2\langle \psi_{n00}, V(\boldsymbol{x})^2 \psi_{n00} \rangle = \frac{4}{n^3}. \tag{2.12}$$

In the appendix of [33] this statement was proven for $n = 1$. The general proof for arbitrary $n$ may be carried out exactly along the same line. Therefore, we obtain the following new upper and lower bounds:

$$P_{lw}(\psi_{n00}) = 1 - \left\{ \frac{2}{n^{3/2}}\tau + \frac{4}{b(\tau)^2 - 1/n^2}\frac{1}{n^{3/2}} + \frac{1}{n\sqrt{3}}\frac{2|b(\tau)|}{b(\tau)^2 - 1/n^2} \right\}^2 \tag{2.13}$$

$$P_{uw}(\psi_{n00}) = \left\{ \frac{2}{n^{3/2}}\tau + \frac{|c(\tau)|}{n\sqrt{3}} + n\sqrt{\frac{5n^2+1}{6}}|b(\tau)| \right\}^2 \tag{2.14}$$

which are weaker than (2.11) and (2.10), in the sense that

$$P_{lw}(\psi_{n00}) \leqslant P_l(\psi_{n00}) \leqslant P(\psi_{n00}) \leqslant P_u(\psi_{n00}) \leqslant P_{uw}(\psi_{n00}). \tag{2.15}$$

In order for (2.13) to be valid we now have to have $b(\tau)^2 > 1/n^2$. We will now turn to a detailed analysis of these bounds by looking at different types of pulses. Our main purpose in the present manuscript for considering states of the type $\psi_{nlm}$ with $n \neq 0$ is to extend our discussion to pulses with longer duration, see also section 2.3. The reason that longer pulse durations are accessible for states with higher $n$ is the $n$ dependence in estimate (2.12) and its effect in (2.14) and (2.13).

### *2.1. Static field*

This is the simplest case, but still instructive to investigate since it already contains the general feature which we will observe for more complicated pulses. It is also important to study, because it may be viewed as the background which is present in most experimental set-ups, before more complicated pulses can be generated. For a static field of intensity $I = E_0^2$ we trivially have

$$E(t) = E_0 \qquad b(t) = E_0 t \qquad c(t) = \tfrac{1}{2} E_0 t^2 \tag{2.16}$$

for $0 \leqslant t \leqslant \tau$. Inserting these functions into (2.10) we may easily compute the upper and lower bound. Here the one-dimensional integrals over time, appearing in (2.11) and (2.10), were carried out numerically. The result is presented in figure 2, which shows that a bound for higher intensities always corresponds to a higher ionization probability. The overall qualitative behaviour clearly indicates that for increasing field strength the ionization probability also increases and tends to one. In particular, curves for different intensities never cross each other. Surely the shown pulse lengths are too short to be realistic and we will indicate below how to obtain situations in which conclusive statements may be drawn concerning longer pulse durations. In the following we will always encounter the same qualitative behaviour.

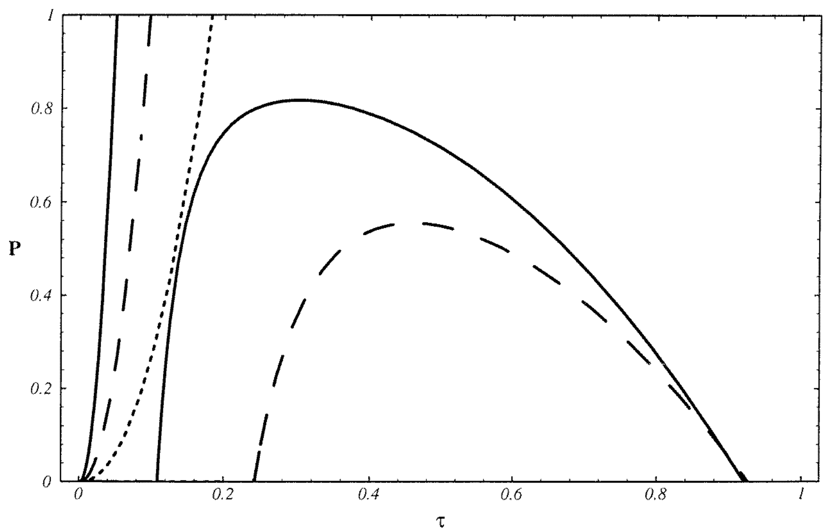


**Figure 2.** Upper (three curves on the left) and lower bound ($P_l$ and $P_u$) for the ionization probability of the $\psi_{100}$-state through a static laser field $E_0$. The dotted curve corresponds to $E_0 = 5$ au, the broken curve to $E_0 = 10$ au and the full curve to $E_0 = 20$ au. The time is in au.

### *2.2. Linearly polarized monochromatic light (LPML)*

Now we have

$$E(t) = E_0 \sin(\omega t) \qquad b(t) = \frac{2E_0}{\omega} \sin^2\left(\tfrac{1}{2}\omega t\right) \qquad c(t) = \frac{E_0}{\omega^2}(\omega t - \sin(\omega t)) \tag{2.17}$$

for $0 \leqslant t \leqslant \tau$. The result of the computation which employs these functions in order to compute (2.10) and (2.11) is illustrated in figure 3. Once again our bounds indicate that for increasing field strength the ionization probability also increases. Keeping the field strength fixed at $E_0 = 2$ au, a comparison between the case for $\omega = 0.4$ and $\omega = 4$ shows (figure 4), as expected, the lower bounds for the ionization probability to be decreasing functions of the frequency. The peak on the left-hand side, which seems to contradict this statement for

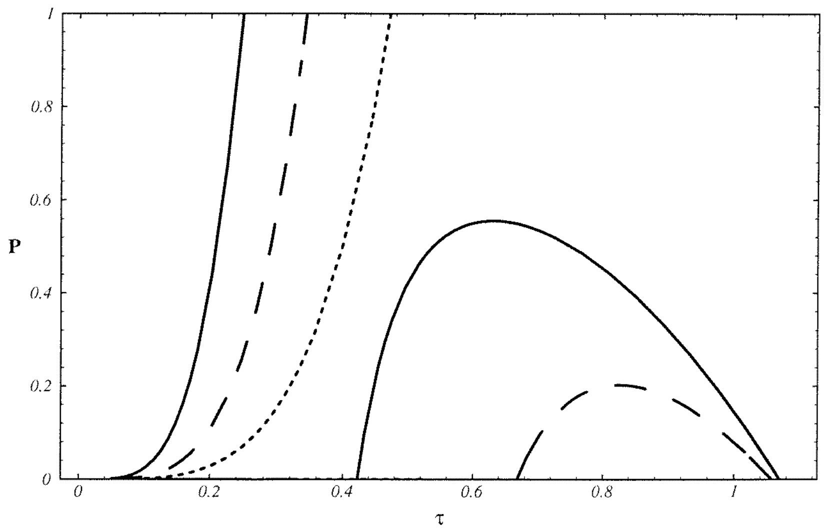


**Figure 3.** Upper (three curves on the left) and lower bound ($P_l$ and $P_u$) for the ionization probability of the $\psi_{100}$-state through a linearly polarized monochromatic laser field $E(t) = E_0 \sin(\omega t)$; $\omega = 1.5$ au. The dotted curve corresponds to $E_0 = 5$ au, the broken curve to $E_0 = 10$ au and the full curve to $E_0 = 20$ au. The time is in au.

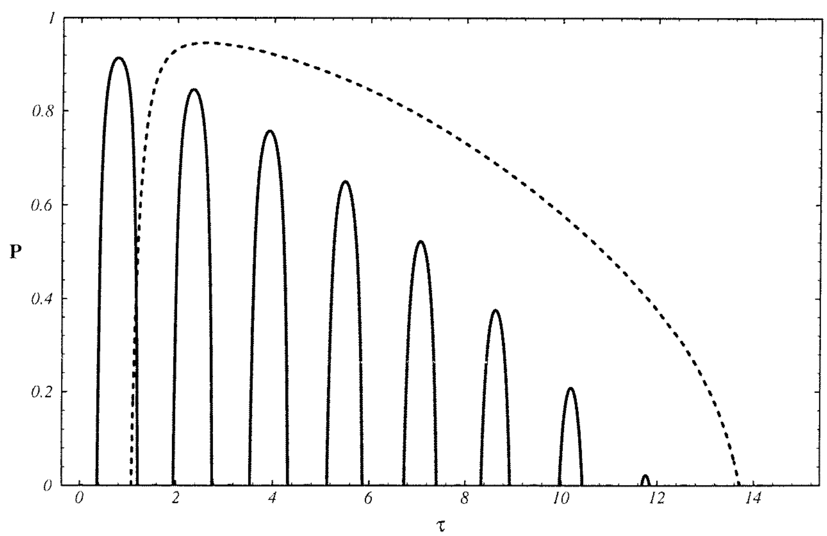


**Figure 4.** Lower bound ($P_{lw}$) for the ionization probability of the $\psi_{10\,00}$-state through a linearly polarized monochromatic laser field $E(t) = E_0 \sin(\omega t)$, $E_0 = 2$ au. The dotted curve corresponds to $\omega = 0.4$ au and the full curve to $\omega = 4$ au. The time is in au.

that region, is only due to the fact that the expression for the lower bound is not valid for $\omega = 0.4$ in that regime. Clearly, this is not what is meant by stabilization, since for this to happen we require fixed frequencies and we have to analyse the behaviour for varying field strengths. The claim [14, 20] is that, in general, very high frequencies are required for this phenomenon to emerge. Our analysis does not support stabilization for any frequency. As

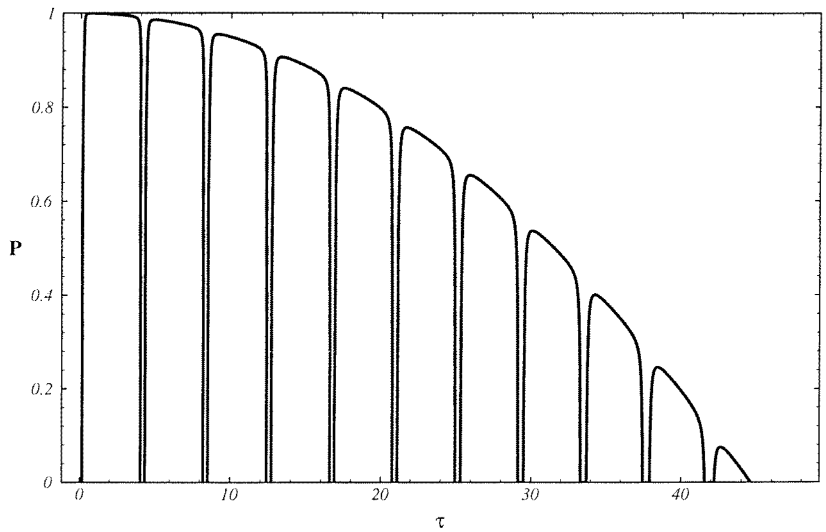


**Figure 5.** Lower bound for the ionization ($P_{lw}$) probability of the $\psi_{20\,00}$-state through a linearly polarized monochromatic laser field $E(t) = E_0 \sin(\omega t)$, $\omega = 1.5$ au, $E_0 = 20$ au. The time is in au.

mentioned above, the shortcoming of the analysis of the bounds $P_u(\psi_{100})$ and $P_l(\psi_{100})$ is that we only see an effect for times smaller than one atomic unit. Figures 4 and 5 also show that, by considering $P(\psi_{n00})$ for higher values of $n$, our expressions also allow conclusions for longer pulse durations. For the reasons mentioned above, in this analysis we employed the slightly weaker bounds (2.14) and (2.13).

### *2.3. LPML with a trapezoidal enveloping function*

We now turn to the simplest case of a pulse which is adiabatically switched on and off. This type of pulse is of special interest since many authors claim [8, 14] that stabilization only occurs in these cases. We consider a pulse of duration $\tau_0$ which has linear turn-on and turn-off ramps of length $T$. Then

$$E(t) = E_0 \sin(\omega t) \begin{cases} t/T & \text{for} \quad 0 \leqslant t \leqslant T \\ 1 & \text{for} \quad T < t < (\tau_0 - T) \\ (\tau_0 - t)/T & \text{for} \quad (\tau_0 - T) \leqslant t \leqslant \tau_0 \end{cases} \tag{2.18}$$

$$b(\tau_0) = \frac{E_0}{\omega^2 T}\{\sin(\omega T) - \sin(\omega\tau_0) + \sin(\omega(\tau_0 - T))\} \tag{2.19}$$

$$\begin{aligned} c(\tau_0) = \frac{E_0}{\omega^3 T}&(2 - 2\cos(\omega T) + 2\cos(\omega\tau_0) - 2\cos(\omega(\tau_0 - T)) \\ &-\omega T \sin(\omega T) + \omega\tau_0 \sin(\omega T) + \omega T \sin(\omega(\tau_0 - T))). \end{aligned} \tag{2.20}$$

The expressions for $b(t)$ and $c(t)$ are rather messy and will not be reported here since we only analyse the weaker bounds. Notice that now, in contrast to the previous cases, both $b(\tau_0)$ and $c(\tau_0)$ may become zero for certain pulse durations and ramps. We shall comment on this situation in section 3. We choose the ramps to be of the form $T = \left(m + \frac{1}{4}\right)2\pi/\omega$ ($m$ being an integer) for the lower and $T = \left(m + \frac{1}{2}\right)2\pi/\omega$ for the upper bound. Our lower

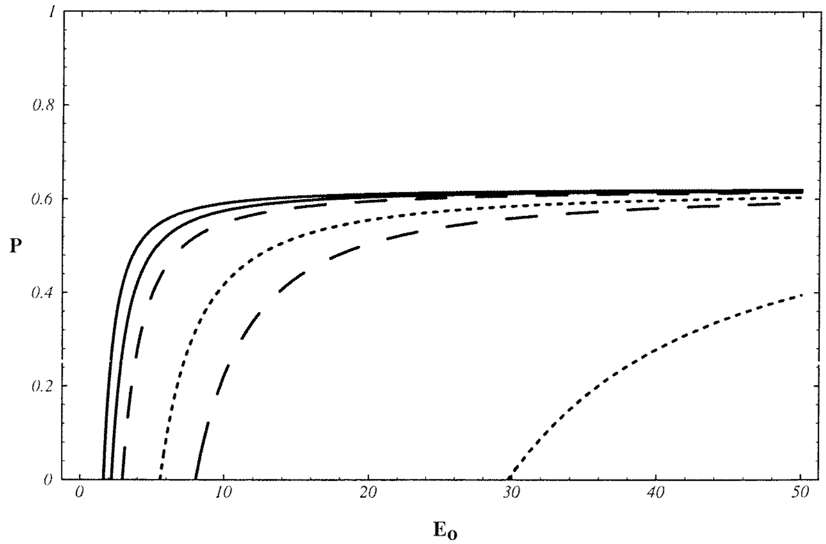


**Figure 6.** Lower bound ($P_{lw}$) for the ionization probability of the $\psi_{34\,00}$-state through a linearly polarized monochromatic laser field with a trapezoidal and a sine-squared turn-on and turn-off enveloping function: the upper and lower curve are of the same line type, respectively (full curve, $\frac{5}{4}$–12–$\frac{5}{4}$ pulse, broken curve, $\frac{9}{4}$–10–$\frac{9}{4}$ pulse and dotted curve, $\frac{17}{4}$–6–$\frac{17}{4}$ pulse), $\omega = 1.5$ au.

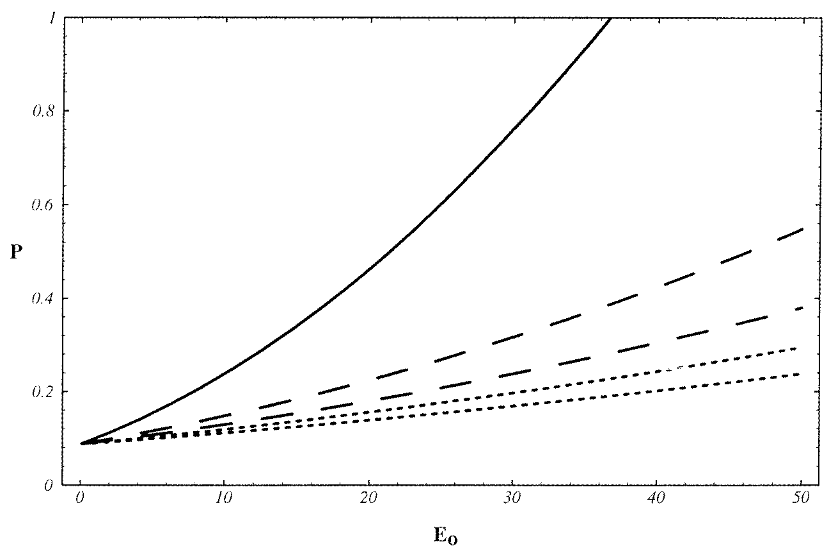


**Figure 7.** Upper bound ($P_{lw}$) for the ionization probability of the $\psi_{34\,00}$-state through a linearly polarized monochromatic laser field with a trapezoidal and a sine-squared turn-on and turn-off enveloping function, upper and lower curve of the same line type, respectively (full curve, $\frac{1}{2}$–6–$\frac{1}{2}$ pulse, broken curve, $\frac{3}{2}$–4–$\frac{3}{2}$ pulse and dotted curve, $\frac{5}{2}$–2–$\frac{5}{2}$ pulse), $\omega = 1.5$ au.

bound does not permit the analysis of half cycles since then $b(\tau_0) = 0$. The results are shown in figures 6 and 7, which both do not show any evidence of stabilization. They further indicate that a decrease in the slopes of the ramps with fixed pulse duration leads to a smaller ionization probability. Once more (we do not present a figure for this, since one may also see this from the analytical expressions), an increase in the frequency leads to a decrease in the lower bound of the ionization probability for fixed field strength.

*2.4. LPML with a sine-squared enveloping function*

Here we consider

$$E(t) = E_0 \sin^2(\Omega t)\sin(\omega t) \tag{2.21}$$

$$\begin{aligned} b(t) = \frac{E_0}{16\omega\Omega^2 - 4\omega^3}\big(&8\Omega^2 + 2\omega^2\cos(\omega t) - 8\Omega^2\cos(\omega t) \\ &-\omega^2\cos((\omega - 2\Omega)t) - 2\omega\Omega\cos((\omega - 2\Omega)t) \\ &-\omega^2\cos((\omega + 2\Omega)t) + 2\omega\Omega\cos((\omega + 2\Omega)t)\big) \end{aligned} \tag{2.22}$$

$$\begin{aligned} c(t) = \frac{E_0}{4\omega^2(\omega - 2\Omega)^2(\omega + 2\Omega)^2}\big(&-8\omega^3\Omega^2 t + 32\omega\Omega^4 t - 2\omega^4\sin(\omega t) \\ &+16\omega^2\Omega^2\sin(\omega t) - 32\Omega^4\sin(\omega t) - \omega^4\sin((2\Omega - \omega)t) \\ &-4\omega^3\Omega\sin((2\Omega - \omega)t) - 4\omega^2\Omega^2\sin((2\Omega - \omega)t) \\ &+\omega^4\sin((\omega + 2\Omega)t) - 4\omega^3\Omega\sin((\omega + 2\Omega)t) + 4\omega^2\Omega^2\sin((\omega + 2\Omega)t)\big) \end{aligned} \tag{2.23}$$

for $0 \leqslant t \leqslant \tau$. At first sight it appears that both $b(t)$ and $c(t)$ are singular at $\omega = \pm 2\Omega$, which, of course, is not the case since both functions are bounded as one may easily derive. With the help of the Schwarz inequality it follows that always $|b(t)| \leqslant t^{1/2}\|I_p\|$ and $|c(t)| \leqslant \frac{1}{2}t^{3/2}\|I_p\|$. We first investigate the situation in which this pulse is switched on smoothly but turned off abruptly. Figure 8 shows that the bounds become nontrivial for times larger than one atomic unit in the same fashion as in the previous cases by considering $P_l(\psi_{n00})$ for higher values of $n$. Figure 9 shows that also in this case the

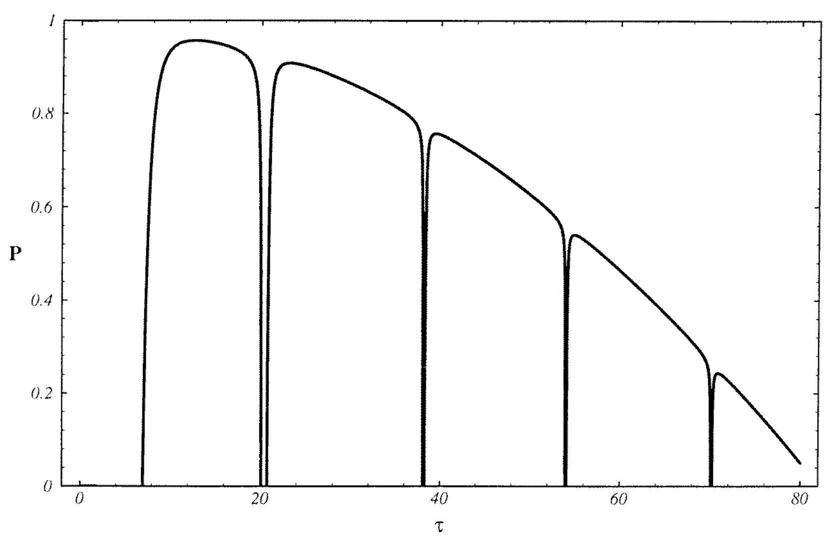


**Figure 8.** Lower bound ($P_{lw}$) for the ionization probability of the $\psi_{30\,00}$-state through a linearly polarized monochromatic laser field with a sine-squared enveloping function $E(t) = E_0\sin(\omega t)\sin(\Omega t)^2$, $\omega = 0.2$ au, $\Omega = 0.01$ au, $E_0 = 20$ au. The time is in au.

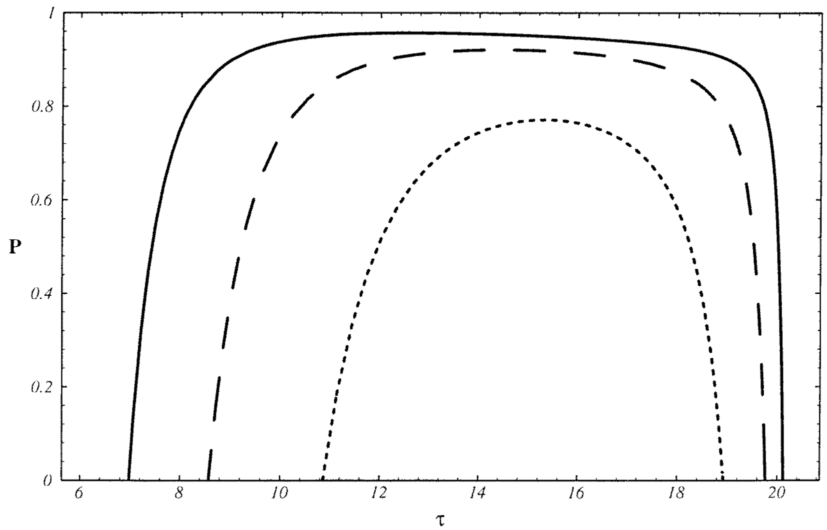


**Figure 9.** Lower bound ($P_{lw}$) for the ionization probability of the $\psi_{30\,00}$-state through a linearly polarized monochromatic laser field with a sine-squared enveloping function $E(t) = E_0 \sin(\omega t) \sin(\Omega t)^2$, $\omega = 0.2$ au, $\Omega = 0.01$ au. The dotted curve corresponds to $E_0 = 5$ au, the broken curve to $E_0 = 10$ au and the full curve to $E_0 = 20$ au. The time is in au.

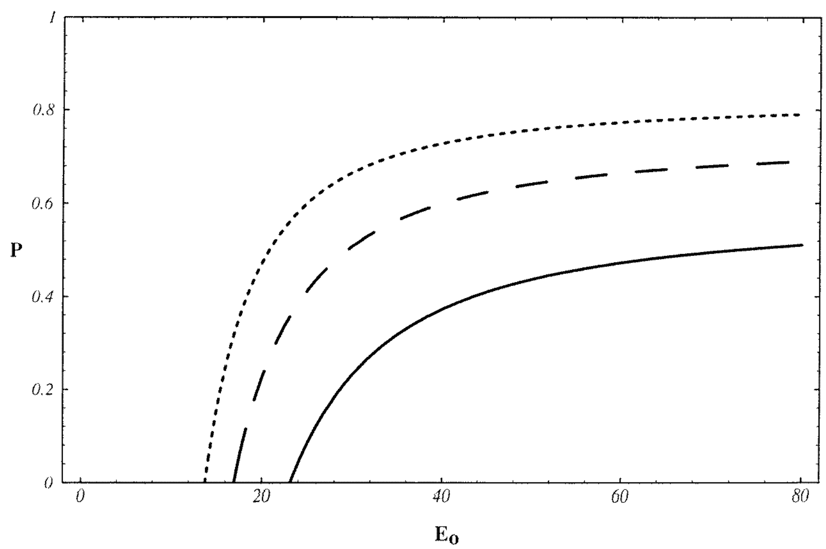


**Figure 10.** Lower bound ($P_{lw}$) for the ionization probability of the $\psi_{n00}$-state through a linearly polarized monochromatic laser field with a sine-squared enveloping function $E(t) = E_0 \sin(\omega t) \sin(\Omega t)^2$, $\omega = 0.8$ au, $\Omega = \omega/13.5$ au. The dotted curve corresponds to $n = 40$, the broken curve to $n = 35$ and the full curve to $n = 30$.

ionization probability tends to one and no sign of stabilization is found. Figure 10 shows the lower bound in which the pulse length is taken to be a half cycle of the enveloping function. Once more it indicates increasing ionization probability with increasing field strength and also for increasing values for $n$. Now following Geltman [10] and Su *et al*

[14] we employ the sine-square only for the turn-on and off and include a plateau region into the pulse shape. Then

$$E(t) = E_0 \sin(\omega t) \begin{cases} \sin^2(\pi t/2T) & \text{for} \quad 0 \leqslant t \leqslant T \\ 1 & \text{for} \quad T < t < (\tau_0 - T) \\ \sin^2(\pi(\tau_0 - t)/2T) & \text{for} \quad (\tau_0 - T) \leqslant t \leqslant \tau_0 \end{cases} \tag{2.24}$$

$$b(\tau_0) = \frac{E_0 \pi^2 (1 + \cos(\omega T) - \cos(\omega(T - \tau_0)) - \cos(\omega \tau_0))}{2\omega\pi^2 - 2\omega^3 T^2} \tag{2.25}$$

$$\begin{aligned} c(\tau_0) = \frac{E_0 \pi^2 2\omega^2}{(\pi^2 - \omega^2 T^2)^2} \big( & \omega\pi^2\tau_0 - \omega^3 T^2 \tau_0 - \omega\pi^2 T \cos(\omega T) + \omega^3 T^3 \cos(\omega T) \\ & + \omega\pi^2 \tau_0 \cos(\omega T) - \omega^3 T^2 \tau_0 \cos(\omega T) - \omega\pi^2 T \cos(\omega(T - \tau_0)) \\ & + \omega^3 T^3 \cos(\omega(T - \tau_0)) + \pi^2 \sin(\omega T) - 3\omega^2 T^2 \sin(\omega T) \\ & + \pi^2 \sin(\omega(T - \tau_0)) - 3\omega^2 T^2 \sin(\omega(T - \tau_0)) - \pi^2 \sin(\omega\tau_0) \\ & + 3\omega^2 T^2 \sin(\omega\tau_0) \big). \end{aligned} \tag{2.26}$$

(Also in these cases the apparent poles in $b(\tau_0)$ and $c(\tau_0)$ for $\omega = \pm\pi/T$ are accompanied by zeros.) The results of these computations are shown in figures 6 and 7, once more with no evidence for bound-state stabilization. A comparison with the linear switch on and off shows that the ionization probability for sine-squared turn-on and offs is lower. The effect is larger for longer ramps.

## 3. Conclusions

We have investigated the ionization probability for the hydrogen atom when exposed to ultra-intense short-pulsed laser radiation of various types of pulse shapes. In comparison with [33], we extended our analysis to the situation which is applicable to any bound-state $\psi_{nlm}$ and, in particular, for the $\psi_{100}$-state we carried out the computation until the end for the stronger upper (2.4) and lower (2.5) bounds. We overcome the shortcoming of [33] which did not allow definite statements for pulses of durations longer than one atomic unit by investigating the bounds for higher values of $n$. A direct comparison between existing numerical computations for small $n$, in particular $n = 1$, and reasonably long pulse durations, is at present not feasible. As our computations show (see also [39]) there is, of course, a quantitatively different behaviour for different values of $n$. However, qualitatively we obtain the same behaviour (refer to figure 10) and therefore we do not consider this to be of any physical significance. Furthermore, from arguments in [42] it follows that precisely the higher Rydberg states are more likely to show any stabilization. Also in [39] it was observed that the ionization probability decreases with increasing principal quantum number for certain pulse shapes. It would be very interesting to carry our analysis further and also investigate the effect resulting from varying $l$ and $m$, in order to compare with [39, 40]. In principle our equations already allow such an analysis, but due to the sum in (A.7) the explicit expressions will be rather messy and we will therefore omit them here.

For the situation when the total classical momentum transfer $b(\tau)$ and the total classical displacement $c(\tau)$ are non-vanishing, we confirm once more the results of [33] and do not find any evidence for bound-state stabilization for ultra-short pulses. This holds for various types of pulses, whether they are switched on (and off), smoothly or not. We therefore agree with Geltman in the conclusion that smooth pulses, in general, will only prolong the onset of ionization but will not provide a mechanism for stabilization.

There is however a particular way of switching on and off, such that $b(\tau) = 0$, but $c(\tau) \neq 0$. These types of pulses are used for instance in [8, 14]. Unfortunately, our bounds do not permit us to make any definite statement about this case, since the lower bound is not applicable (in the sense that then the necessary condition $\frac{1}{2}b^2(\tau) > -E$ for the validity of the lower bound is not fulfilled) and the upper bound gives for typical values of the frequency and field strength ionization probabilities larger than one. So, in principle, for these types of pulses the possibility of bound-state stabilization remains. It would be very interesting to find alternative expressions for the upper and lower bounds which allow conclusions for this case.

For the case $b(\tau) = c(\tau) = 0$ the upper bound $P_u$ remains an increasing function of the field strength due to the properties of the Hilbert space norm of the difference of the potential in the Kramers–Henneberger frame and in the laboratory frame applied to the state $\psi_{100}$. The weaker upper bound takes on the value $P_{uw}(\psi_{n00}) = 4\tau^2/n^3$, which at first sight seems counterintuitive, since it implies that the upper bound decreases with increasing $n$, i.e. for states close to the ionization threshold, and fixed $\tau$. Classically this may, however, be understood easily. For closed Kepler orbits, i.e. ellipses, with energies sufficiently close to zero (depending on $\tau$), for any pulse with small $b(\tau)$ and $c(\tau)$, these quantities will be very close to the actual changes, caused by the pulse, of the momentum and the coordinate, respectively. So in this case ionization, i.e. the transition to a hyperbolic or parabolic orbit will therefore be very unlikely. Also in the investigations in [42] stabilization is found for this case. A detailed analysis [43] allowing for all possible values of $b(\tau)$ and $c(\tau)$ using entirely different methods confirms the results of the present manuscript and our previous investigations [33, 42].

## Acknowledgments

We would like to thank J H Eberly, S Geltman and V Kostrykin for very useful discussions and correspondence. One of the authors (CFMF) is supported by the DAAD.

## Appendix

In this appendix we will provide the explicit calculation of the term

$$N^2(\boldsymbol{y}, \psi) = \langle \psi, V(\boldsymbol{x})^2 \psi \rangle + \langle \psi, V(\boldsymbol{x}-\boldsymbol{y})^2 \psi \rangle - 2\langle \psi, V(\boldsymbol{x}-\boldsymbol{y})\, V(\boldsymbol{x}) \psi \rangle. \tag{A.1}$$

For $\psi = \psi_{nlm}$ the first term is well known to be equal to $1/\left[n^3\left(l+\frac{1}{2}\right)\right]$ [34]. We did not find a computation for the matrix element involving the Coulomb potential in the Kramers–Henneberger frame in the literature and will therefore present it here. Starting with the familiar expansion of the shifted Coulomb potential in terms of spherical harmonics

$$\frac{1}{|\boldsymbol{x}-\boldsymbol{y}|} = \sum_{l=0}^{\infty} \left(\frac{r_<^l}{r_>^{l+1}}\right) \sqrt{\frac{4\pi}{2l+1}}\, Y_{l0}(\vartheta, \phi) \tag{A.2}$$

where $r_< = \min(|\boldsymbol{x}|, |\boldsymbol{y}|)$ and $r_> = \max(|\boldsymbol{x}|, |\boldsymbol{y}|)$, we obtain

$$\begin{aligned} \langle \Psi_{nlm} \big| |\boldsymbol{x}-\boldsymbol{y}|^{-1} |\boldsymbol{x}|^{-1} \big| \Psi_{nlm} \rangle &= \sum_{l'=0}^{\infty} \int \mathrm{d}\Omega\, Y_{lm}^*\, Y_{l'0}\, Y_{lm} \sqrt{\frac{4\pi}{2l'+1}} \\ &\quad \times \left( \int_0^{|\boldsymbol{y}|} \mathrm{d}r \left(\frac{r}{|\boldsymbol{y}|}\right)^{l'+1} R_{nl}^2 + \int_{|\boldsymbol{y}|}^{\infty} \mathrm{d}r \left(\frac{|\boldsymbol{y}|}{r}\right)^{l'} R_{nl}^2 \right) \end{aligned} \tag{A.3}$$

which by the well known formula from angular momentum theory

$$\int \mathrm{d}\Omega\, Y^*_{lm}\, Y_{l_1m_1}\, Y_{l_2m_2} = \sqrt{\frac{(2l_1+1)(2l_2+1)}{4\pi(2l+1)}}\langle l_1l_2;\,00|l0\rangle\langle l_1l_2;\,m_1m_2|lm\rangle \tag{A.4}$$

leads to

$$\sum_{l'=0}^{\infty}\langle ll';\,00|l0\rangle\langle ll';\,m0|lm\rangle\left(\int_0^{|\boldsymbol{y}|}\mathrm{d}r\left(\frac{r}{|\boldsymbol{y}|}\right)^{l'+1}R^2_{nl}+\int_{|\boldsymbol{y}|}^{\infty}\mathrm{d}r\left(\frac{|\boldsymbol{y}|}{r}\right)^{l'}R^2_{nl}\right) \tag{A.5}$$

for (A.3). Here $\langle l_1l_2;\,m_1m_2|lm\rangle$ denote the Wigner or Clebsch–Gordan coefficients in the usual conventions (see e.g. [41]).

We shall now consider the term

$$\big\langle\Psi_{nlm}\big||\boldsymbol{x}-\boldsymbol{y}|^{-2}\big|\Psi_{nlm}\big\rangle. \tag{A.6}$$

Employing (A.2) and the formula

$$Y_{l_1m_1}Y_{l_2m_2} = \sqrt{\frac{(2l_1+1)(2l_2+1)}{4\pi}}\sum_{l'm'}\frac{1}{(2l'+1)}Y_{l'm'}\langle l_1l_2;\,m_1m_2|l'm'\rangle\langle l_1l_2;\,00|l'0\rangle$$

yields

$$\frac{1}{|\boldsymbol{x}-\boldsymbol{y}|^2} = \sum_{k,l'}\sum_{\tilde{l}=|k-l'|}^{|k+l'|}\frac{r_<^{k+l'}}{r_>^{k+l'+2}}\sqrt{\frac{4\pi}{2\tilde{l}+1}}\langle kl';\,00|\tilde{l}0\rangle^2 Y_{\tilde{l}0}. \tag{A.7}$$

Once again applying (A.4) shows that (A.6) equals

$$\sum_{\tilde{l},\bar{l},l'}\langle\tilde{l}l';\,00|\tilde{l}0\rangle^2\langle\bar{l}l;\,0m|lm\rangle\langle\bar{l}l;\,00;\,l0\rangle\left(\int_0^{|\boldsymbol{y}|}\mathrm{d}r\left(\frac{r}{|\boldsymbol{y}|}\right)^{l'+\tilde{l}+2}R^2_{nl}+\int_{|\boldsymbol{y}|}^{\infty}\mathrm{d}r\left(\frac{|\boldsymbol{y}|}{r}\right)^{l'+\tilde{l}}R^2_{nl}\right). \tag{A.8}$$

For s-states, i.e. $l=0$, we may carry out the sums over the Clebsch–Gordan coefficients easily. In (A.5) the only contribution comes from $l'=0$ and we trivially obtain

$$\big\langle\Psi_{n00}\big||\boldsymbol{x}-\boldsymbol{y}|^{-1}|\boldsymbol{x}|^{-1}\big|\Psi_{n00}\big\rangle = \int_0^{|\boldsymbol{y}|}\mathrm{d}r\,\frac{r}{|\boldsymbol{y}|}R^2_{n0}+\int_{|\boldsymbol{y}|}^{\infty}\mathrm{d}r\,R^2_{n0}. \tag{A.9}$$

In (A.8) the sum over $\bar{l}$ contributes only for $\bar{l}=0$ and together with $\langle\tilde{l}l';\,00|00\rangle^2 = \delta_{\tilde{l}l'}/(2\tilde{l}+1)$ it leads to

$$\big\langle\Psi_{n00}\big||\boldsymbol{x}-\boldsymbol{y}|^{-2}\big|\Psi_{n00}\big\rangle = \sum_{l=0}^{\infty}\frac{1}{2l+1}\left(\int_0^{|\boldsymbol{y}|}\mathrm{d}r\left(\frac{r}{|\boldsymbol{y}|}\right)^{2l+2}R^2_{nl}+\int_{|\boldsymbol{y}|}^{\infty}\mathrm{d}r\left(\frac{|\boldsymbol{y}|}{r}\right)^{2l}R^2_{nl}\right). \tag{A.10}$$

We turn to the case $n=1$ (with $\Psi_{100}=\big(2/\sqrt{4\pi}\,\big)\mathrm{e}^{-|\boldsymbol{x}|}$) for which (A.5) becomes

$$\big\langle\Psi_{100}\big||\boldsymbol{x}-\boldsymbol{y}|^{-1}|\boldsymbol{x}|^{-1}\big|\Psi_{100}\big\rangle = \frac{1-\mathrm{e}^{-2|\boldsymbol{y}|}}{|\boldsymbol{y}|}. \tag{A.11}$$

As a consistency check one may consider the asymptotic behaviours $|\boldsymbol{y}|\to\infty$ and $|\boldsymbol{y}|\to 0$, which give, as expected, 0 and 2, respectively. Using the series expansion for the logarithm, equation (A.10) for $n=1$ becomes

$$\big\langle\Psi_{100}\big||\boldsymbol{x}-\boldsymbol{y}|^{-2}\big|\Psi_{100}\big\rangle = \frac{2}{|\boldsymbol{y}|}\left(\int_0^{|\boldsymbol{y}|}\mathrm{d}r\,\ln\left(\frac{|\boldsymbol{y}|+r}{|\boldsymbol{y}|-r}\right)r\mathrm{e}^{-2r}+\int_{|\boldsymbol{y}|}^{\infty}\mathrm{d}r\,\ln\left(\frac{r+|\boldsymbol{y}|}{r-|\boldsymbol{y}|}\right)r\mathrm{e}^{-2r}\right). \tag{A.12}$$

Then using the integrals

$$\int \mathrm{d}r\ \ln(1 \pm r) r \mathrm{e}^{-2cr} = \frac{1}{4c^2}\Big((1 \mp 2c)\mathrm{e}^{\pm 2cr}\,\mathrm{Ei}(\mp 2c(1 \pm r)) - \mathrm{e}^{-2cr}(1 + (1 + 2cr)\ln(1 \pm r))\Big) \tag{A.13}$$

$$\int \mathrm{d}r\ \ln\left(1 \pm r^{-1}\right) r \mathrm{e}^{-2cr} = \frac{1}{4c^2}\Big((1 \mp 2c)\mathrm{e}^{\pm 2cr}\,\mathrm{Ei}(2c(\mp 1 - r)) - \mathrm{Ei}(-2cr) - (1 + 2cr)\mathrm{e}^{-2cr}\ln\left(1 \pm r^{-1}\right)\Big) \tag{A.14}$$

we obtain

$$\left\langle \Psi_{n00} \middle| |\boldsymbol{x} - \boldsymbol{y}/2|^{-2} \middle| \Psi_{n00} \right\rangle = \left(1 - |\boldsymbol{y}|^{-1}\right)\mathrm{e}^{-|\boldsymbol{y}|}\,\mathrm{Ei}(|\boldsymbol{y}|) + \left(1 - |\boldsymbol{y}|^{-1}\right)\mathrm{e}^{|\boldsymbol{y}|}\,\mathrm{Ei}(-|\boldsymbol{y}|). \tag{A.15}$$

As a consistency check we may again consider the asymptotic behaviour, that is $|\boldsymbol{y}| \to 0$ and $|\boldsymbol{y}| \to \infty$, which gives correctly 2 and 0, respectively. Assembling now (A.1), (A.11) and (A.15) gives as claimed (2.8). In the same fashion one may also compute $N(\boldsymbol{y}, \psi_{nlm})$ for arbitrary $n, l$ and $m$.

## References

[1] Lambropoulos P 1972 *Phys. Rev. Lett.* **29** 453
[2] Rudolph W and Wilhelmi B 1989 *Light Pulse Compression* (London: Harwood)
[3] Gordon W 1926 *Z. Phys.* **40** 117
Volkov D M 1935 *Z. Phys.* **94** 250
[4] Keldysh L V 1965 *Sov. Phys.–JETP* **20** 1307
Perelomov A M, Popov V S and Terentev M V 1966 *Sov. Phys.–JETP* **23** 924
Perelomov A M, Popov V S and Terentev M V 1967 *Sov. Phys.–JETP* **24** 207
Faisal F H M 1973 *J. Phys. B: At. Mol. Phys.* **6** L89
[5] Geltman S and Teague M R 1974 *J. Phys. B: At. Mol. Phys.* **7** L22
[6] Reiss H R 1980 *Phys. Rev.* A **22** 1786
Reiss H R 1997 *Laser Phys.* **7** 543
[7] Geltman S 1992 *Phys. Rev.* A **45** 5293
[8] Grobe R and Fedorov M V 1992 *Phys. Rev. Lett.* **68** 2592
Grobe R and Fedorov M V 1993 *J. Phys. B: At. Mol. Opt. Phys.* **26** 1181
[9] Geltman S 1994 *J. Phys. B: At. Mol. Opt. Phys.* **27** 257
[10] Geltman S 1994 *J. Phys. B: At. Mol. Opt. Phys.* **27** 1497
[11] Collins L A and Merts A L 1988 *Phys. Rev.* A **37** 2415
[12] Bardsley J N, Szöke A and Comella M J 1988 *J. Phys. B: At. Mol. Opt. Phys.* **21** 3899
[13] LaGattuta K J 1989 *Phys. Rev.* A **40** 683
[14] Javanainen J, Eberly J H and Su Q 1988 *Phys. Rev.* A **38** 3430
Javanainen J, Eberly J H and Su Q 1990 *Phys. Rev. Lett.* **64** 862
Su Q and Eberly J H 1990 *J. Opt. Soc. Am.* B **7** 564
Law C K, Su Q and Eberly J H 1991 *Phys. Rev.* **44** 7844
Su Q and Eberly J H 1991 *Phys. Rev.* A **43** 2474
Su Q 1993 *Laser Phys.* **2** 241
Su Q, Irving B P, Johnson C W and Eberly J H 1996 *J. Phys. B: At. Mol. Opt. Phys.* **29** 5755
Su Q, Irving B P and Eberly J H 1997 *Laser Phys.* **7** 568
[15] Reed V C and Burnett K 1990 *Phys. Rev.* A **42** 3152
Reed V C and Burnett K 1991 *Phys. Rev.* A **43** 6217
[16] Latinne O, Joachain C J and Dörr M 1994 *Europhys. Lett.* **26** 333
Dörr M, Latinne O and Joachain C J 1995 *Phys. Rev.* **52** 4289
[17] Shirley J H 1965 *Phys. Rev.* B **138** 979
[18] Potvliege R M and Shakeshaft R 1988 *Phys. Rev.* A **38** 1098
Potvliege R M and Shakeshaft R 1988 *Phys. Rev.* A **38** 4597
Potvliege R M and Shakeshaft R 1988 *Phys. Rev.* A **38** 6190
Potvliege R M and Shakeshaft R 1990 *Phys. Rev.* A **40** 4061

Dörr M, Potvliege R M, Proulx D and Shakeshaft R 1991 *Phys. Rev.* A **43** 3729
Dörr M, Burke P G, Joachain C J, Noble C J, Purvis J and Terao-Dunseath M 1993 *J. Phys. B: At. Mol. Opt. Phys.* **25** L275
[19] Dimou L and Faisal F H M 1993 *Acta Phys. Polon.* A **86** 201
Dimou L and Faisal F H M 1994 *Phys. Rev.* A **46** 4564
Faisal F H M, Dimou L, Stiemke H-J and Nurhuda M 1995 *J. Nonlin. Opt. Phys. Mater.* **4** 701
[20] Gavrila M and Kaminski J Z 1984 *Phys. Rev. Lett.* **52** 613
Offerhaus M J, Kaminski J Z and Gavrila M 1985 *Phys. Lett.* **112A** 151
Gavrila M, Offerhaus M J and Kaminski J Z 1986 *Phys. Lett.* **118A** 331
Pont M, Offerhaus M J and Gavrila M 1988 *Z. Phys.* D **9** 297
van de Ree J, Kaminski J Z and Gavrila M 1988 *Phys. Rev.* A **37** 4536
Pont M, Walet N R, Gavrila M and McCurdy C W 1988 *Phys. Rev. Lett.* **61** 939
Pont M and Gavrila M 1990 *Phys. Rev. Lett.* **65** 2362
[21] Leopold J G and Parcival I C 1978 *Phys. Rev. Lett.* **41** 944
Grochmalicki J, Lewenstein M and Rzażewski K 1991 *Phys. Rev. Lett.* **66** 1038
Grobe R and Law C K 1991 *Phys. Rev.* A **44** 4114
Benvenuto F, Casati G and Stepelyanski D L 1992 *Phys. Rev.* A **45** R7670
Menis S, Taieb R, Veniard V and Maquet A 1992 *J. Phys. B: At. Mol. Opt. Phys.* **25** L263
Dombrowski M, Rosenberger A T and Sung C C 1995 *Phys. Lett.* **199A** 204
Rosenberger A T, Sung C C, Pethel S D and Bowden C M 1997 *Laser Phys.* **7** 563
[22] Tikhonova O V and Fedorov M V 1997 *Laser Phys.* **7** 574
[23] Burnett K, Reed V C and Knight P L 1993 *J. Phys. B: At. Mol. Opt. Phys.* **26** 561
[24] Eberly J H and Kulander K C 1993 *Science* **262** 1229
[25] Delone N B and Krainov V P 1994 *Multiphoton Processes in Atoms* (Berlin: Springer) ch 10
[26] Geltman S 1995 *Chem. Phys. Lett.* **237** 286
[27] Chen Q and Bernstein I B 1993 *Phys. Rev.* A **47** 4099
[28] Krainov V P and Preobrazenski M A 1993 *Sov. Phys.–JETP* **76** 559
[29] de Boer M P, Hoogenraad J H, Vrijen R B, Noordam L D and Muller H G 1993 *Phys. Rev. Lett.* **71** 3263
de Boer M P, Hoogenraad J H, Vrijen R B and Noordam L D 1994 *Phys. Rev.* A **50** 4133
[30] Enss V, Kostrykin V and Schrader R 1995 *Phys. Rev.* A **50** 1578
[31] Kostrykin V and Schrader R 1995 *J. Phys. B: At. Mol. Opt. Phys.* **28** L87
[32] Kostrykin V and Schrader R 1997 Ionization of atoms and molecules by short strong laser pulses *J. Phys. A: Math. Gen.* **30** 265
[33] Fring A, Kostrykin V and Schrader R 1996 *J. Phys. B: At. Mol. Opt. Phys.* **29** 5651
[34] Bethe H A and Salpeter E E 1957 *Quantum Mechanics of One and Two-Electron Atoms* (Berlin: Springer)
Landau L D and Lifschitz E M 1977 *Quantum Mechanics* (New York: Pergamon)
[35] Cycon H L, Froese R G, Kirsch W and Simon B 1987 *Schrödinger Operators* (Berlin: Springer)
[36] Reed M and Simon B 1972 *Methods of Modern Mathematical Physics* vol 2 (New York: Academic)
[37] Kramers H A 1956 *Collected Scientific Papers* (Amsterdam: North-Holland)
[38] Henneberger W C 1968 *Phys. Rev. Lett.* **21** 838
[39] Pont M and Shakeshaft R 1991 *Phys. Rev.* A **44** R4110
[40] Wójcik A, Parzyński R and Grudka A 1997 *Phys. Rev.* A **55** 2144
Parzyński R and Wójcik A 1997 *Laser Phys.* **7** 551
[41] Inui Y, Tanabe Y and Onodera Y 1996 *Group Theory and its Application in Physics* (Berlin: Springer)
[42] Fring A, Kostrykin V and Schrader R 1997 Ionization probabilities through ultra-intense fields in the extreme limit *J. Phys. A: Math. Gen.* **30** 8599
[43] Figueira de Morisson Faria C, Fring A and Schrader R Momentum transfer, displacement and stabilization in preparation